

NOTES

Gassed Power Draw of Mixed Impeller Systems

KEVIN J. MYERS¹ and MOLLY I. RUSSELL

Chemical & Materials Engineering, University of Dayton, Dayton, OH 45469-0246, U.S.A.

and

ANDRÉ BAKKER

Chemineer, Inc., Dayton, OH 45401-1123, U.S.A.

A technique is proposed to predict the gassed power draw of mixed impeller systems as a weighted average of the gassed power draws of the individual impellers. The success of this method requires determining the gassed power draws of the individual impellers in the proper gassed environment. In the case of the upper impellers, this environment is provided by a rubber membrane sparger that distributes the gas evenly over the vessel cross section. Extensive comparisons of experimental gassed power draws of mixed impeller systems with model predictions verify the accuracy of the proposed technique.

On propose une technique afin de prédire la consommation de puissance en milieu aéré de systèmes de turbines multiples comme une moyenne pondérée de la consommation de puissance en milieu aéré des turbines individuelles. Pour réussir, cette méthode nécessite qu'on détermine les consommations de puissance en milieu aéré des turbines individuelles dans l'environnement d'aération approprié. Dans le cas des turbines supérieures, cet environnement est fourni par un aérateur à membrane de caoutchouc qui distribue le gaz de manière égale au-dessus de la section transversale du réservoir. Des comparaisons extensives entre les consommations de puissance en milieu aéré expérimentales des systèmes de turbines multiples et des prédictions du modèle démontrent la précision de la technique proposée.

Keywords: gas-liquid agitation, power draw, mixed impeller systems.

Many industrial vessels are designed with aspect ratios significantly greater than one ($Z/T > 1$). This is particularly common for large volume gas-liquid reactors such as fermenters. Agitation of these tall reactors is challenging, requiring multiple impellers. Use of multiple radial-flow impellers has been the typical design approach, but these impeller systems are less than optimal. Their primary deficiency is that they do not provide adequate top-to-bottom mixing because of the zoning that occurs, with each individual impeller establishing its own zone of influence. The slow exchange of material between these zones leads to poor reactor performance when uniform distribution of reactants, dissolved gases, or nutrients is critical.

To overcome the poor blending characteristics of multiple radial-flow impeller systems, high-solidity axial-flow gas dispersion impellers have been developed. Although these impellers provide improved blending, they are also subject to torque and flow instabilities that limit their application (McFarlane and Nienow, 1995). Özcan-Taskin et al. (1995) have found that stable gas dispersion can be obtained with up-pumping axial-flow impellers, but this approach has not been widely applied industrially.

One strategy that has been successfully applied in numerous industrial installations is the use of mixed impeller systems. These impeller systems combine a lower gas-dispersing impeller with upper axial-flow impellers to provide both stable gas dispersion and rapid top-to-bottom blending. These mixed impeller systems have been shown to have gassed blend times that are less than half those of radial-flow impeller systems while providing the same mass transfer capabilities at equal gassing rates and gassed power inputs (Myers et al., 1994).

Despite their industrial importance, there is little power draw data available for mixed impeller systems. Eliezer (1987) studied mixed Rushton turbine/high-efficiency impeller systems, but the aeration numbers (N_A) were limited to a maximum value of 0.03, below the range of interest for most industrial applications. Kuboi and Nienow (1982) reported the power draw characteristics of mixed impeller systems using pitched-blade turbines as the upper impellers. However, they studied pitched-blade turbines in the up-pumping mode of operation, rather than in the down-pumping mode of operation of interest in this work.

Gassed power draw prediction

Prediction of gassed power draw in agitated systems has been the subject of much research. Bruijn et al. (1974) and Nienow and Wisdom (1974) were able to relate the gassed power draw of single impellers to the cavity structure behind the impeller blades. However, as Hicks and Gates (1976) pointed out, the environment experienced by an upper impeller in multiple-impeller systems is quite different than that of the lowest, gas-dispersing impeller. Based on the assumption that very little gas passes directly through the upper impellers, Nienow and Lilly (1979) suggested that any drop in power draw due to gassing of upper impellers was solely the result of the decreased density of the gas-liquid mixture. They found that this approach yielded reasonable predictions of the gassed power draw of dual Rushton impeller systems. However, the later study of Kuboi and Nienow (1982) did not support this elementary approach to the problem.

The approach adopted here is to separately determine the gassed power draw of the dispersing and upper impellers in the appropriate environment, then to combine this information to predict the gassed power draw of the mixed impeller

¹Author to whom correspondence may be addressed. E-mail address: kmyers1@engr.udayton.edu

system. This leads to the following prediction of the relative gassed power draw of the mixed impeller system.

$$\left(\frac{P_g}{P_o}\right)_{\text{mixed}} = \alpha \left(\frac{P_g}{P_o}\right)_{\text{dispersing}} + (1-\alpha) \left(\frac{P_g}{P_o}\right)_{\text{upper}} \quad \dots \quad (1)$$

α is not an adjustable model fitting parameter; rather, it is the fraction of the ungassed power drawn by the dispersing impeller which can be determined a priori from the diameters and ungassed power numbers of the dispersing and upper impellers.

$$\alpha = \frac{(P_o)_{\text{dispersing}}}{(P_o)_{\text{dispersing}} + (P_o)_{\text{upper}}} \quad \dots \quad (2)$$

In terms of the ungassed impeller power numbers, N_p , and diameters, D , this expression becomes

$$\alpha = \frac{(N_p D^5)_{\text{dispersing}}}{(N_p D^5)_{\text{dispersing}} + (n N_p D^5)_{\text{upper}}} \quad \dots \quad (3)$$

where n represents the number of upper impellers. It has been assumed that the upper impellers are all of the same type and size, although in practice this is not always the case.

The question remains as to the proper environment in which to determine the gassed power draws of the dispersing and upper impellers for use in Equation (1). Ideally, a shaft with multiple strain gauges would be used so that the power draw of each impeller in a multiple-impeller system could be measured individually. This, however, is not always possible, and the method used here involves measuring the power draw of each impeller as a single impeller, adjusting the gas environment/sparging method to mimic the conditions in a gassed vessel with multiple impellers. For the dispersing impeller, the relative gassed power draw is simply measured at the speed and gassing rate of interest in the absence of the upper impellers. The upper impellers should be studied at the same speed and gassing rate as the dispersing impeller, but the choice of appropriate environment is not as clear. As shown in Figure 1, the relative gassed power draw of axial-flow impellers is very sensitive to sparging technique (the data of Figure 1 was taken as part of the current study, using the apparatus and techniques described in the following section). This is due to the sensitivity of the power draw of these impellers to the head against which they must pump.

For sparge rings with diameters equal to or smaller than the impeller diameter, the relative gassed power draw of an axial-flow impeller is low at low gassing rates and increases with increasing gassing rate. This is due to the ability of the impeller to disperse the gas at low flows such that the gas rises along the wall of the vessel rather than through the impeller. This reinforces the flow pattern of the impeller, decreasing its power draw. As the gas flow is increased, the ability of the impeller to disperse the gas is impaired. This leads to gas directly loading the impeller, acting against the impeller's pumping action, and causing increased power draw (Bakker, 1992). These small ring spargers do not provide an environment that simulates the environment experienced by the upper impellers in a mixed impeller system when the dispersing impeller is dispersing the incoming gas. However,

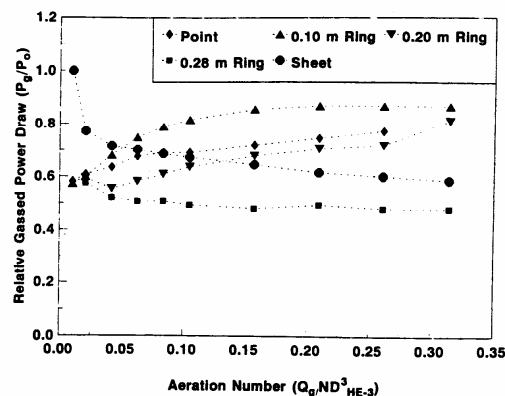


Figure 1 — The influence of sparge technique on the relative gassed power draw of the HE-3 impeller ($D_{HE-3} = 0.203$ m, $D_{HE-3}/T = 0.508$).

this information may be useful if the dispersing impeller is flooded and gas flow impinges directly on the upper impellers.

The two sparging methods that are most likely to simulate the environment experienced by the upper impellers in a mixed impeller system are the sheet sparger and the large sparge ring. The sheet sparger is designed to provide uniform dispersion of the gas over the entire vessel cross section. Nocentini et al. (1988) found this sparging technique yielded good estimates of the gassed power draw of upper radial-flow impellers in multiple radial-flow impeller systems (Nocentini et al. actually used a spiral sparger rather than a sheet, but the idea of dispersing the gas over the vessel cross section is the same). This approach is also likely to be suitable for studying the relative gassed power draw of upper, axial-flow impellers in mixed impeller systems. However, at low gas flows this technique may not be the best method available. At low gas flows, the dispersing impeller drives most of the gas to the wall region. Gas rising near the vessel wall reinforces the flow pattern of the upper impellers, reducing their relative gassed power draws. A large ring sparger simulates this behavior at low gas flows, as illustrated in Figure 1. This data demonstrates that the relative gassed power draw of an axial-flow impeller at low gassing rates is much lower when it is sparged with a large ring ($D_s = 1.38 D$) than when it is sparged with a sheet. The difference in relative gassed power draw of these two sparging techniques decreases at higher gassing rates. Russell (1995) was unable to find significant differences between the ability of these two sparging methods to predict the gassed power draw of mixed impeller systems, so only the results obtained with the sheet sparger technique will be presented here. Russell (1995) also found that the ungassed power draw of mixed impeller systems was essentially equal to the sum of the ungassed power draws of the individual impellers if the impeller separation was equal to at least the diameter of the largest impeller in the system.

Experimental apparatus and procedure

Experiments were performed with air and tap water in an acrylic dished-bottom vessel with an internal diameter of 0.400 m and a straight side of 1.22 m. The vessel was equipped

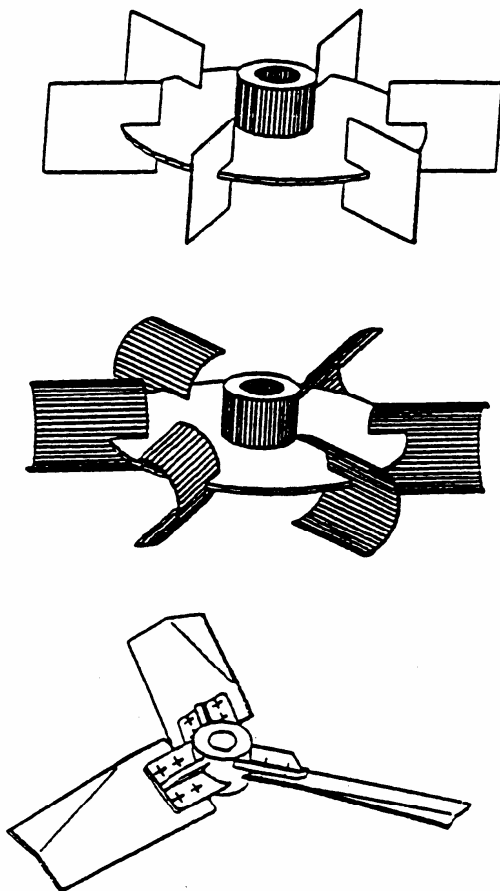


Figure 2 — Impellers studied: D-6 (top), CD-6 (middle), and HE-3 (bottom).

with four stainless steel vertical baffles that were spaced at 90° intervals around the vessel periphery. The baffles extended the length of the straight side, were 0.033 m wide, and were offset from the vessel wall by 0.005 m. When studying mixed impeller systems, gas was introduced to the vessel through a 0.102-m diameter circular sparge ring that was centered in the vessel 0.064 m above the lowest point of the vessel base. The ten equally-spaced holes of the sparge ring, each of 0.0032 m diameter, were directed downward.

The impellers studied are shown in Figure 2 (all impellers were supplied by Chemineer, Inc., Dayton, OH). Two dispersing impellers, Chemineer's D-6 and CD-6 turbines, were investigated. Both of these impellers are six-bladed, disc-style turbines. The D-6 impeller has flat blades, while the CD-6 has semicircular blades that are designed to provide improved gas-handling characteristics. The diameter of the dispersing impeller was held constant at 0.160 m ($D_{D-6}/T = D_{CD-6}/T = 0.400$). The dispersing impeller disc diameters were 0.102 m, while the dispersing impellers had blade widths/heights of 0.0350 m and blade lengths of 0.0462 m. An off-bottom clearance of 0.102 m was used for all dispersing impellers. The only upper impeller studied was Chemineer's HE-3, which was of standard construction. The

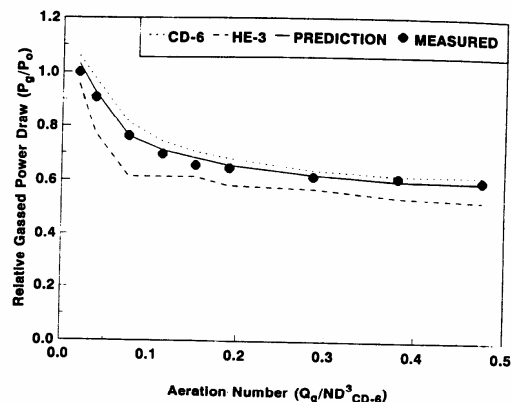


Figure 3 — Comparison of experimental and predicted relative gassed power draws of a dual CD-6/HE-3 impeller system at a Froude number of 0.6 ($D_{CD-6} = 0.160$ m, $D_{CD-6}/T = 0.400$, $D_{HE-3} = 0.203$ m, $D_{HE-3}/T = 0.508$, $\alpha = 0.75$; Froude and aeration numbers based on the CD-6 diameter).

HE-3 is a three-bladed, high-efficiency impeller that generates a highly-axial flow. HE-3 diameters of 0.165, 0.203, and 0.241 m ($D_{HE-3}/T = 0.413$, 0.508, and 0.603) were used. The HE-3 impellers were studied only in the down-pumping mode. All impeller blades and discs had a thickness of 0.0015 m, and all impeller hubs had a bore (corresponding to the shaft diameter) of 0.0127 m. The turbulent power numbers required to calculate the power split parameter α from Equation (3) are 0.28 for the HE-3, 2.8 for the CD-6, and 5.5 for the D-6. Small variations (less than ten percent) in the turbulent power number of the HE-3 due to varying impeller diameter to tank diameter ratio (D/T) have been neglected.

Mixed impeller systems with two (one dispersing and one upper) and four (one dispersing and three upper) impellers were investigated. The impeller separation in all instances was 0.200 m ($S = T/2$). The ungassed liquid level was 0.480 m for the dual-impeller system and 0.800 m for the four-impeller system ($Z_o/T = 1.2$ and 2.0, respectively).

When determining the relative gassed power draws of the individual impellers for use in Equation (1), the dispersing impellers were studied in the system described above, except that the upper impellers were not present. The relative gassed power draw of the upper impellers was determined using a perforated neoprene sheet sparger that distributed the gas uniformly over the cross section of the vessel.

Rotational speeds in the range of 2.5 to 10 s^{-1} and volumetric gas flows in the range of 4.7×10^{-4} to 1.4×10^{-2} $m^3(actual)/s$ were investigated. Rotational speeds were measured with a zero velocity magnetic pickup and gas flows were measured with calibrated rotameters. A calibrated strain gauge reaction torque sensor (Lebow model 2404-100) yielded torque measurements that were conditioned (Daytronics model 9171) to provide an accuracy of better than five percent. All data sets were taken at a constant rotational speed with varying gas flow rate.

Results and discussion

Figure 3 compares model predictions with experimental data taken with a dual CD-6/HE-3 impeller system at a Froude number of 0.6. The Froude ($N_{Fr} = N^2 D/g$) and aeration ($N_A = Q_g/ND^3$) numbers of mixed impeller systems are

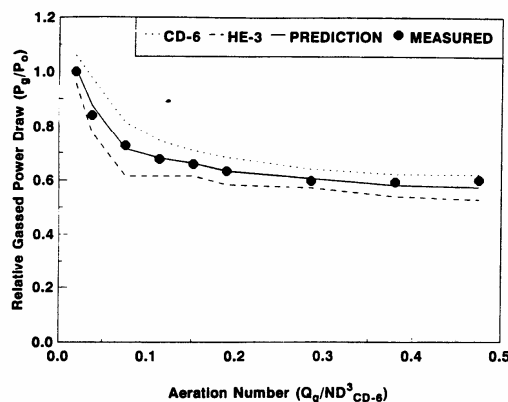


Figure 4 — Comparison of experimental and predicted relative gassed power draws of a four CD-6/HE-3 impeller system at a Froude number of 0.6 ($D_{CD-6} = 0.160$ m, $D_{CD-6}/T = 0.400$, $D_{HE-3} = 0.203$ m, $D_{HE-3}/T = 0.508$, $\alpha = 0.50$; Froude and aeration numbers based on the CD-6 diameter).

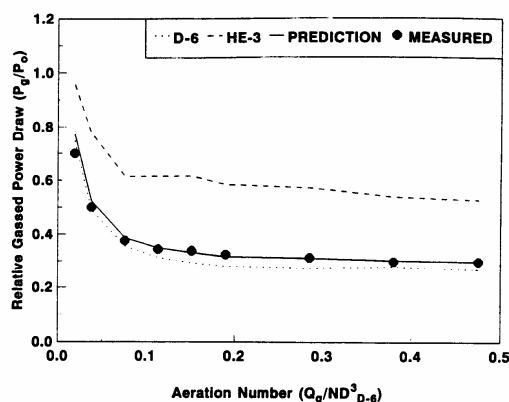


Figure 6 — Comparison of experimental and predicted relative gassed power draws of a dual D-6/HE-3 impeller system at a Froude number of 0.6 ($D_{D-6} = 0.160$ m, $D_{D-6}/T = 0.400$, $D_{HE-3} = 0.203$ m, $D_{HE-3}/T = 0.508$, $\alpha = 0.86$; Froude and aeration numbers based on the D-6 diameter).

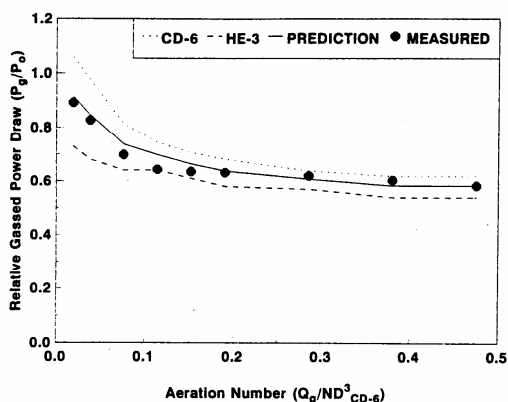


Figure 5 — Comparison of experimental and predicted relative gassed power draws of a dual CD-6/HE-3 impeller system at a Froude number of 0.6 ($D_{CD-6} = 0.160$ m, $D_{CD-6}/T = 0.400$, $D_{HE-3} = 0.241$ m, $D_{HE-3}/T = 0.603$, $\alpha = 0.56$; Froude and aeration numbers based on the CD-6 diameter).

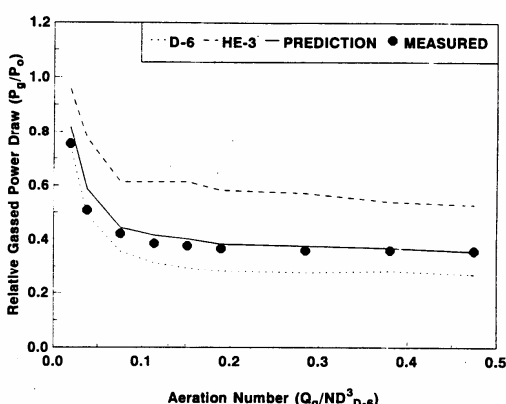


Figure 7 — Comparison of experimental and predicted relative gassed power draws of a four D-6/HE-3 impeller system at a Froude number of 0.6 ($D_{D-6} = 0.160$ m, $D_{D-6}/T = 0.400$, $D_{HE-3} = 0.203$ m, $D_{HE-3}/T = 0.508$, $\alpha = 0.66$; Froude and aeration numbers based on the D-6 diameter).

based upon the diameter of the dispersing impeller (the CD-6 in this case). For legibility of the figures, the experimental CD-6 relative gassed power draw is presented as a dotted line without data points, the HE-3 relative gassed power draw as measured using the sheet sparger is presented as a dashed line, and the model prediction is presented as a solid line. The CD-6 diameter is 0.160 m ($D_{CD-6}/T = 0.400$), while that of the HE-3 is 0.203 m ($D_{HE-3}/T = 0.508$). These impeller diameters correspond to a value of 0.75 for the power split parameter α . The model predictions can be seen to be accurate, and an average error of three percent was observed for this dual-impeller system for data taken at Froude numbers of 0.3, 0.45, 0.6, and 0.9 (Russell, 1995).

The experimental relative gassed power draw of a four-impeller system (a 0.160 m CD-6 ($D_{CD-6}/T = 0.400$) and three 0.203 m HE-3s ($D_{HE-3}/T = 0.508$)) is compared with model predictions in Figure 4. The power split parameter α is 0.5 in this instance. The model predictions are accurate,

with an average error less than five percent for data taken at Froude numbers of 0.3, 0.45, 0.6, and 0.9 (Russell, 1995).

To vary the power split between the lower dispersing impeller and the upper impeller(s) in mixed impeller systems, the diameters of the impellers are adjusted. The data of Figure 5 was taken with a dual-impeller system with a 0.160 m CD-6 ($D_{CD-6}/T = 0.400$) and a 0.241 m HE-3 ($D_{HE-3}/T = 0.603$) at a Froude number of 0.6. These diameters correspond to a power split parameter α of 0.56, and the average error of the model predictions is just over three percent. Model predictions also compare well with data taken with a smaller HE-3 (0.165 m, $D_{HE-3}/T = 0.413$), exhibiting an average error of less than two percent (this data is not shown in a figure). In this instance the power split parameter α is 0.90.

Figures 6 and 7 illustrate that model predictions of mixed D-6/HE-3 impeller systems are also accurate. The Froude number is 0.6, the D-6 diameter is 0.160 m ($D_{D-6}/T = 0.400$), and the HE-3 diameter is 0.203 m ($D_{HE-3}/T = 0.508$). The

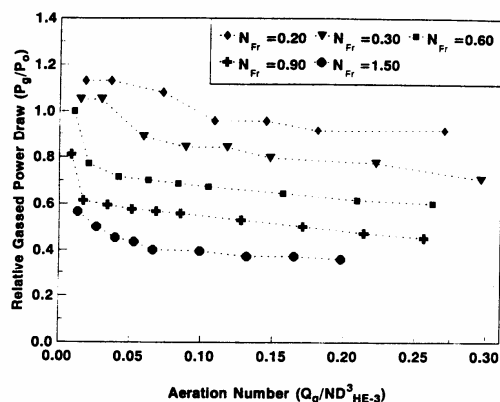


Figure 8 — The influence of Froude and aeration numbers on the relative gassed power draw of the HE-3 impeller ($D_{HE-3} = 0.203$ m, $D_{HE-3}/T = 0.508$; Froude and aeration numbers based on the HE-3 diameter).

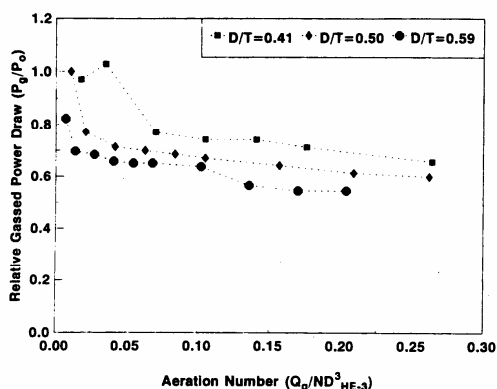


Figure 9 — The influence of impeller diameter to tank diameter ratio on the relative gassed power draw of the HE-3 impeller at a Froude number of 0.6 (Froude and aeration numbers based on the HE-3 diameter).

magnitude of the power split parameter α is 0.86 for the dual-impeller system and 0.66 for the four-impeller system. These high α values are due to the high ungassed power number of the D-6 impeller. The very low relative gassed power draws of the D-6 are also evident in Figures 6 and 7.

A review of all of the comparisons of experimental data and model predictions of the gassed power draw of mixed impeller systems (Figures 3 through 7) indicates that a precise value of the power split parameter α is not required. Good accuracy should be obtained with any reasonable estimate of this model parameter.

It has been demonstrated that the proposed method provides an accurate technique to predict the gassed power draw of mixed impeller systems. The only data that is required is the ungassed impeller power numbers and the gassed power draws of the individual impellers in the appropriate environments. This data is typically available for dispersing impellers, but not for the upper impellers. Figure 8

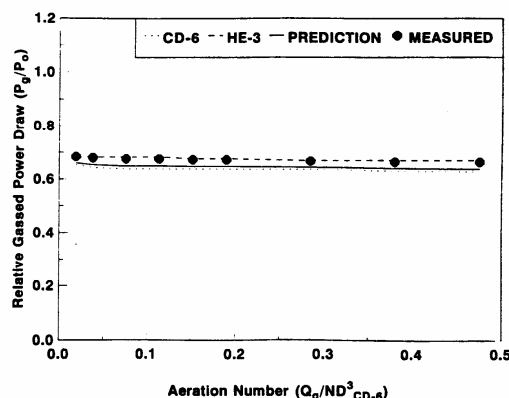


Figure 10 — Comparison of experimental and predicted relative gassed power draws of a dual CD-6/HE-3 impeller system at a Froude number of 0.6 in a viscous liquid ($\mu = 0.45$ Pa·s, $D_{CD-6} = 0.160$ m, $D_{CD-6}/T = 0.400$, $D_{HE-3} = 0.203$ m, $D_{HE-3}/T = 0.508$, $\alpha = 0.75$; Froude and aeration numbers based on the CD-6 diameter).

provides the necessary data for the HE-3 impeller. The data was obtained in an air-water dispersion using the sheet sparger technique with an impeller diameter to tank diameter ratio of approximately fifty percent ($D_{HE-3}/T = 0.508$). This data is typical of most impellers, with the relative gassed power draw decreasing with increases in either the aeration or Froude numbers. The data of Figure 9, taken at a Froude number of 0.6, demonstrates that the impeller diameter to tank diameter ratio has a significant influence on the relative gassed power draw of the HE-3 impeller. As the impeller diameter increases, more of the dispersed gas passes through the volume swept out by the impeller, leading to a decreased relative gassed power draw. The Froude and aeration numbers of Figures 8 and 9 are based on the HE-3 diameter (unlike the mixed impeller system data of previous figures, in which the aeration and Froude numbers are based on the dispersing impeller diameter).

All preceding data was taken with air-water dispersions, but many fermentations occur in more viscous liquids. One set of data, presented in Figure 10, was taken with a Newtonian aqueous glycerine solution with a viscosity of 0.45 Pa·s. A dual CD-6/HE-3 impeller system was used, with the CD-6 diameter being 0.160 m ($D_{CD-6}/T = 0.400$) and the HE-3 diameter being 0.203 m ($D_{HE-3}/T = 0.508$). The flow was transitional in this instance, with the CD-6 and HE-3 impeller Reynolds numbers ($N_{Re} = ND^2/\nu$) being 410 and 670, respectively. Although the power numbers of both the CD-6 and the HE-3 are slightly higher than their turbulent values, the power split parameter α is essentially unchanged from its turbulent value of 0.75. The Froude number was 0.6 based on the diameter of the CD-6 impeller. The aeration number can be seen to have very little effect on the relative gassed power draw, with large, stable cavities being formed on the impeller blades at even the lowest aeration rates (Nienow and Ulbrecht, 1985). The comparison of data and model predictions in Figure 10 is not a critical test of the model since the dispersing and upper impellers exhibit very similar relative gassed power draws at the conditions studied. However, the model predictions are good in this case and warrant more extensive testing of the proposed method of predicting the gassed power draw of mixed impeller systems in viscous gas dispersion.

Concluding remarks

A technique has been developed to accurately predict the gassed power draw of mixed impeller systems based on the gassed power draws of the individual impellers. The success of the technique relies on determining the gassed power draws of the individual impellers in the appropriate environment. The dispersing impeller should be at the conditions of interest (speed, gassing rate, and sparger configuration) in the absence of any upper impellers. The upper impeller(s) should also be operated at the speed and gassing rate of interest, but the gas should be fed to the system in a manner such that it is distributed over the vessel cross section. This mimics the environment that the upper impellers experience in a mixed impeller system. The use of multiple upper impellers is readily taken into account by weighting the gassed power draw of these impellers by the number of upper impellers in the system. The experimental verification of this gassed power draw prediction technique has been limited to systems in which the impeller spacing is equal to or greater than the diameter of the largest impeller. The technique may not work when closer impeller spacings are used.

Nomenclature

D	= impeller diameter, m
D_s	= sparge ring diameter, m
g	= acceleration of gravity, m/s^2
N	= impeller rotational speed, s^{-1}
N_A	= aeration number, $N_A = Q_g/ND^3$, dimensionless
N_{Fr}	= Froude number, $N_{Fr} = N^2D/g$, dimensionless
N_p	= impeller power number, $N_p = P/\rho N^3 D^5$, dimensionless
N_{Re}	= impeller Reynolds number, $N_{Re} = ND^2/\nu$, dimensionless
n	= number of upper impellers in a mixed impeller system, dimensionless
P	= impeller power draw, W
P_g/P_o	= relative gassed power draw, dimensionless
Q_g	= volumetric gas flow rate, $\text{m}^3(\text{actual})/\text{s}$
S^g	= impeller separation, m
T	= vessel diameter, m
Z	= liquid level, m

Greek letters

α	= power split parameter defined in Equations (2) and (3), dimensionless
ν	= kinematic viscosity, m^2/s
μ	= viscosity, $\text{Pa}\cdot\text{s}$
ρ	= density, kg/m^3

Subscripts

$CD-6$	= refers to the $CD-6$ impeller
$D-6$	= refers to the $D-6$ impeller
$dispersing$	= refers to the dispersing impeller in a mixed impeller system
g	= refers to gassed conditions
$HE-3$	= refers to the $HE-3$ impeller

$mixed$	= refers to a mixed impeller system
o	= refers to ungassed conditions
s	= refers to the sparger
$upper$	= refers to the upper impeller(s) in a mixed impeller system

References

- Bakker, A., "Hydrodynamics of Stirred Gas-Liquid Dispersions", Ph.D. thesis, Delft University of Technology, Delft, The Netherlands (1992).
- Bruijn, W., K. van't Riet and J. M. Smith, "Power Consumption with Aerated Rushton Turbines", *Trans. Inst. Chem. Eng.* **52**, 99-104 (1974).
- Eliezer, E. D., "Power Absorption by New and Hybrid Mixing Systems under Gassed and Ungassed Conditions", in "Biotechnology Processes: Scaleup and Mixing", C. S. Ho and J. Y. Oldshue, ed., American Institute of Chemical Engineers, New York (1987), pp. 22-30.
- Hicks, R. W. and L. E. Gates, "How to Select Turbine Agitators for Dispersing Gas into Liquids", *Chem. Eng.* **83**(14), 141-148 (1976).
- Kuboi, R. and A. W. Nienow, "The Power Drawn by Dual Impeller Systems under Gassed and Ungassed Conditions", in "Proc. Fourth European Conference on Mixing" (organized by BHRA Fluid Engineering, Cranfield, Bedford, England), Noordwijkerhout, The Netherlands, April 27-29 (1982), pp. 247-261.
- McFarlane, C. M. and A. W. Nienow, "Studies of High Solidity Hydrofoil Impellers for Aerated Bioreactors. 1. Review", *Biotechnol. Prog.* **11**, 601-607 (1995).
- Myers, K. J., J. B. Fasano and A. Bakker, "Gas Dispersion Using Mixed High-Efficiency/Disc Impeller Systems", in "Proc. Eighth European Conference on Mixing" (IChemE Symposium Series No. 136), Cambridge, U.K., September 21-23 (1994), pp. 65-72.
- Nienow, A. W. and M. D. Lilly, "Power Drawn by Multiple Impellers in Sparged Agitated Vessels", *Biotechnol. Bioeng.* **21**, 2341-2345 (1979).
- Nienow, A. W. and J. J. Ulbrecht, "Gas-Liquid Mixing in High Viscosity Liquids", in "Mixing of Liquids by Mechanical Agitation", J. J. Ulbrecht and G. K. Patterson, ed., Gordon and Breach, New York (1985), Chpt. 6.
- Nienow, A. W. and D. J. Wisdom, "Flow over Disc Turbine Blades", *Chem. Eng. Sci.* **29**, 1994-1997 (1974).
- Nocentini, M., F. Magelli, G. Pasquali and D. Fajner, "A Fluid-Dynamic Study of a Gas-Liquid, Non-Standard Vessel Stirred by Multiple Impellers", *Chem. Eng. J.* **37**, 53-59 (1988).
- Özcan-Taskin, N. G., F. Fabreguette, R. B. Badham, K. N. Dyster, Z. Jaworski, I. P. T. Moore, A. W. Nienow and J. McKemmie, "A Comparative Study of Aerated Power and the Bulk Blending Characteristics of a Newly Designed Impeller", presented at Mixing XV (15th Biennial North American Mixing Conference), Banff, Alberta, Canada, June 18-23 (1995).
- Russell, M. I., "Gas-Liquid Agitation with Mixed Impeller Systems", M.S. thesis, University of Dayton, Dayton, OH (1995).

Manuscript received August 26, 1996; revised manuscript received January 13, 1997; accepted for publication January 24, 1997.